JLAB-PHY-97-03

A CsI(Na) Based Radiation Detector for High Resolution Imaging Studies Using Iodine 125 in Small Animal Research

Andrew Weisenberger[1], Eric Bradley[2], Stan Majewski[1] and Margaret Saha[2]
[1]Thomas Jefferson National Accelerator Facility, Newport News, VA
[2]Biology Department, College of William and Mary, Williamsburg, VA

ABSTRACT

We report on the development of a high resolution radiation imaging system which is capable of detecting and imaging the coincident gamma and X-ray emissions of the radioisotope iodine 125 (^{125}I). Iodine 125 is commonly available as a radioactive label to tag molecular biology probes. Iodine 125 decays via electron capture emitting a 35 keV gamma-ray with the prompt emission of several 27-32 keV X-rays. A coincidence condition can be set to detect the ^{125}I decays thus reducing background radiation contribution to the image. We are testing the use of arrays of CsI(Na) crystal scintillators coupled to position sensitive photomultiplier tubes for this application. Laboratory studies have thus far been done on mice using a prototype of our detector which is intended to be used to image gene expression in live mice to advance research in neurobiology.

Keywords: x-ray, gamma-ray, imaging, iodine 125, gene imaging and scintillators

1. Introduction

Developmental neurobiology seeks to understand the processes that lead to the development of the various parts and functions of the brain and nervous system. The application of the tools of molecular biology are paramount to advancing neuroscience. Much of molecular biology research deals with attempting to unravel the details of the control of gene expression. It is the instructions encoded in genes, defined by sequences of DNA, that direct the cell to grow, differentiate, function and reproduce.

At present the only methods readily available to follow gene expression and how it controls neural differentiation and function in a developing organism is through *in situ* hybridization and immunochemical assays at single moments in time for an individual organism. One must sacrifice the organism to make a measurement, essentially taking a snap shot of the state of expression of the gene of interest. What is needed is an ability to detect gene expression and receptor binding *in vivo* for a developing organism. To be fully useful the *in vivo* gene imaging technique should be real-time, quantitative and able to follow an organism over several weeks.

1.1 *In Vivo* Gene Detection

There are only a few methods used to follow gene expression in live animals i.e. *in vivo*. One technique was used to identify live transgenic animals utilizes green fluorescent fusion proteins (GFP) to identify live transgenic zebra fish (Peters et al., [1]). A transgenic zebra fish carrying a transgene which expresses GFP could then be detected using UV illumination. The GFP method only works for transparent animals.

When a gene is expressed it first results in the transcription of an mRNA transcript molecule which is then translated into a protein. Anti-sense mRNA probes have been constructed that could be introduced into a live organism. Dewanjee et al., [2, 3, 4] has shown that it is possible to construct and successfully use radiolabeled antisense mRNA probes to detect the target mRNA *in vivo* in mice using a standard gamma camera as the detector system. Dewanjee et al. injected into mammary tumor-bearing BALB/c mice ^{111}In (171.2 keV) radiolabeled antisense and sense mRNA probes. Standard molecular biology techniques were used to construct the RNA probe to achieve hybridization to their target mRNA molecule. The probe was injected into the mice and gamma camera imaging was conducted at several time intervals. They observed high concentration of the probe in the mammary region of the mouse and concluded that the antisense probe could be used for noninvasive imaging of c- *myc* oncogene mRNA for malignant tumors[3]. The gamma camera system they used produced scintiphotographs with resolution of the order of 0.5 cm. Standard gamma cameras are composed of a matrix of small individual photomultiplier tubes (PMT) which are optically coupled to a large NaI scintillating crystal. The locating of the

point of interaction in the crystal is done by a centroid calculation using signals from all of the PMTs. Typically commercial gamma cameras can only achieve a resolution of ~4 mm [5].

Tjuvajev et al.[6] have used radiolabled marker substrates to detect the presence of particular enzymes resulting from the expression of a transduced gene. The researchers used radiolabeled 5-iodo-2'-fluoro-2'-deoxy-1-beta-D-arabinofuranosyluracil as a marker substrate to measure the effectiveness of gene transfer techniques being tested for gene therapy. They used quantitative autoradiography (not high resolution radiation imaging) to measure enhanced regional radioactivity in the regions of the rat's brain that had been the target of the gene therapy. In a later study Tjuvajev et al. [7] used a dual-headed ADAC Genesys gamma camera (ADAC, Milpitas, CA) equipped with a high efficiency, high resolution collimator to do gamma camera imaging and SPECT for gene research involving rats. Again they used the same radiolabeled marker substrates to detect the presence of particular enzymes resulting from the expression of a transduced gene. Their images were reconstructed to a 64 x 64 matrix with 3.9 x 3.9 mm^2 pixels. Clearly this type of research would benefit from high resolution gamma cameras designed specifically for small animal imaging.

1.2 Iodine 125

As mentioned earlier we are investigating the use of radioactive iodine 125 (^{125}I) as the radioactive substance linked to a molecular probe. We intend to follow the progression of gene expression in a live organism by using standard probes linked to the isotope but detected and imaged with a novel type of radiation imaging detector. The radioisotope ^{125}I is commonly used in molecular biology and medical research and is readily available linked to nucleic acids and antibodies from companies providing probes for gene research [8]. Therefore one can easily construct a RNA, DNA or protein probe labeled with ^{125}I. The gamma and x-ray emissions from the decay of ^{125}I though not energetic enough for practical use in medical imaging applications in humans it is sufficient for small animal studies.

Iodine 125 has a half life of ~60 days and decays via electron capture with the emission of a 35 keV gamma-ray with the prompt emission of several 27-32 keV Kα and Kβ shell X-rays from the daughter product ^{125}Te [9]. Because of these correlated phenomena a coincidence condition can be set to detect the ^{125}I decays and thus eliminating any unwanted background radiation. Typical background sources are natural radioactivity present in materials in and around the detectors and cosmic radiation. This background defines the lower limit of detection of the gamma emitter of interest. Therefore, unlike in the cases with single gamma emitters, such as ^{99m}Te, a clear distribution of the ^{125}I isotope in the laboratory animal can be obtained, even if present in minute quantities. This coincidence technique has been shown to be useful for the detection of extremely low concentrations (on the order of attomole) of ^{125}I linked to a probe [10]. Figure 1 shows the decay scheme of ^{125}I which decays to its daughter product ^{125}Te with the emission of a gamma ray.

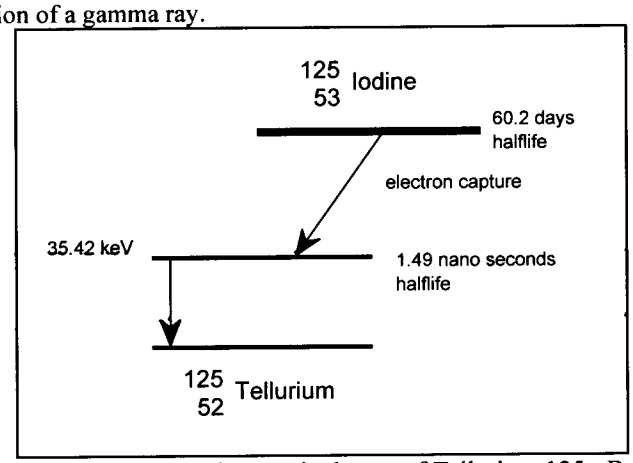

Figure 1. Decay scheme for Iodine 125 to a nuclear excited state of Tellurium 125. Based on Lederer and Shirley [9].

2. Detector System to Image Iodine 125

We have obtained encouraging results with a prototype detector doing coincidence ^{125}I imaging involving mouse studies. The detector was composed of a high resolution collimator and a 60mm x 60mm x 1mm plate of YAP crystal scintillator coupled to a Hamamatsu R2486 position sensitive photomultiplier tube (PSPMT) [11]. The R2486 PSPMT has an active area of about 50 mm in diameter. It has an eleven stage proximity focused parallel dynode mesh structure and 16x16 crossed wire anodes with a pitch of 3.75 mm. An electric potential difference of about 1.2 kV is set between the photocathode and last dynode achieving an electron gain of ~10^6. Incident X-rays

or gamma rays produce scintillation photons in the crystal scintillator. The scintillation photons incident on the face of the PSPMT interact with the photocathode that is on the inner surface of the PSPMT window. Photons induce electron emission from the photocathode through the photoelectric effect. In Figure 2 is a diagram demonstrating how a scintillation photon when incident on the photocathode of the PSPMT results in photoelectrons which then interact with the mesh dynodes thus resulting in a shower of secondary electrons. This shower of electrons is intercepted by the 16x16 crossed wire anodes after being reflected back from the last solid dynode.

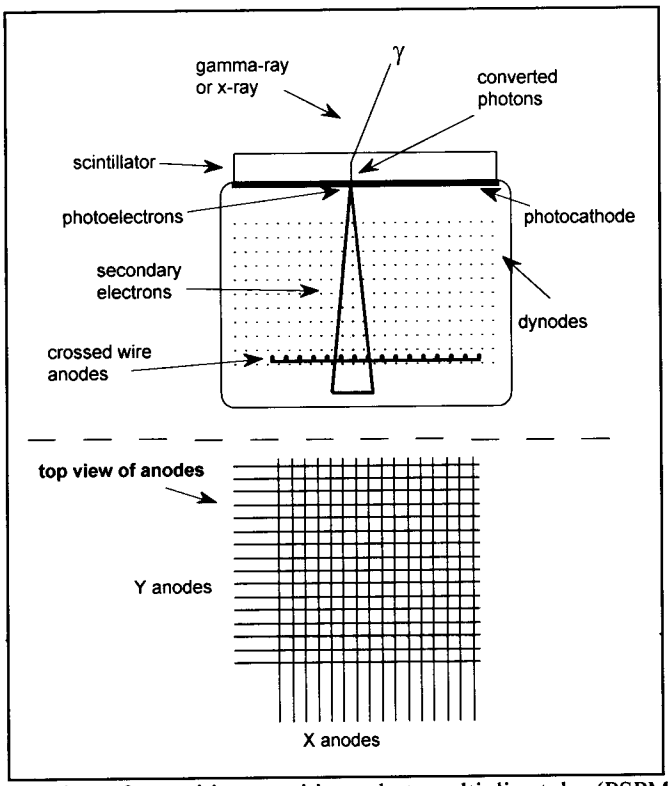

Figure 2. Schematic of the operation of a position sensitive photomultiplier tube (PSPMT) with an eleven stage mesh dynode stack to provide a multiplication of secondary electrons. Incident γ or X-rays induce scintillation photons in the crystal scintillator. Readout of the secondary electron shower is achieved by the 16x16 crossed wire anodes.

Determination of the position of gamma interaction in the scintillator is determined by computing a truncated center of gravity of the signal distribution on the x and y anode sectors of the PSPMT. The calculation of the center of gravity is achieved by using only the digitized signal of those anode wires in the calculation that have a chosen optimum fraction of the sum of the anode signals (typically 5%). We have found that the use of this truncated COG technique is essential to maximizing use of the PSPMT active area [12].

3. CsI(Na) Based Detector System

In order to obtain higher position resolution, a larger imaging area and a distortion free image we have constructed a compact gamma camera using a CsI(Na) scintillating crystal array coupled to the Hamamatsu R3292-02 PSPMT (the 5 inch diameter version of the Hamamatsu 2486). The good performance of pixellated scintillating crystal arrays coupled to PSPMTs has been demonstrated [13]. CsI(Na) has approximately 60% better light yield than YAP. The scintillator array we have tested is 110 mm in diameter and each crystal element is 2.0 x 2.0 mm ^{2} in area and 3 mm thick. This array based detector allows the removal of the image distortion and the correction of the non-uniformity of response common to the Hamamatsu PSPMTs.

3.1 Readout of the Hamamatsu R3292-02 PSPMT

The Hamamatsu R3292-02 PSPMT has 28x28 crossed anode wires. The number of individual channels read out was reduced while still retaining the advantage of local readout (as opposed to integral methods such as current division or delay lines) by connecting anode wires in groups of two wires thus reducing the number of channels to instrument by a factor of two. We have not found a decrease in position resolution by this operation , because lowered granularity of readout was compensated by an improvement in the signal-to-noise ratio. The original 28x+28y anode wire readout was reduced to 14x+14y wire groups. All anode sector signals were amplified in low noise LeCroy TRA 1000 amplifiers and delayed by 50 nsec before entering 28 individual ADC channels (see Figure 3).

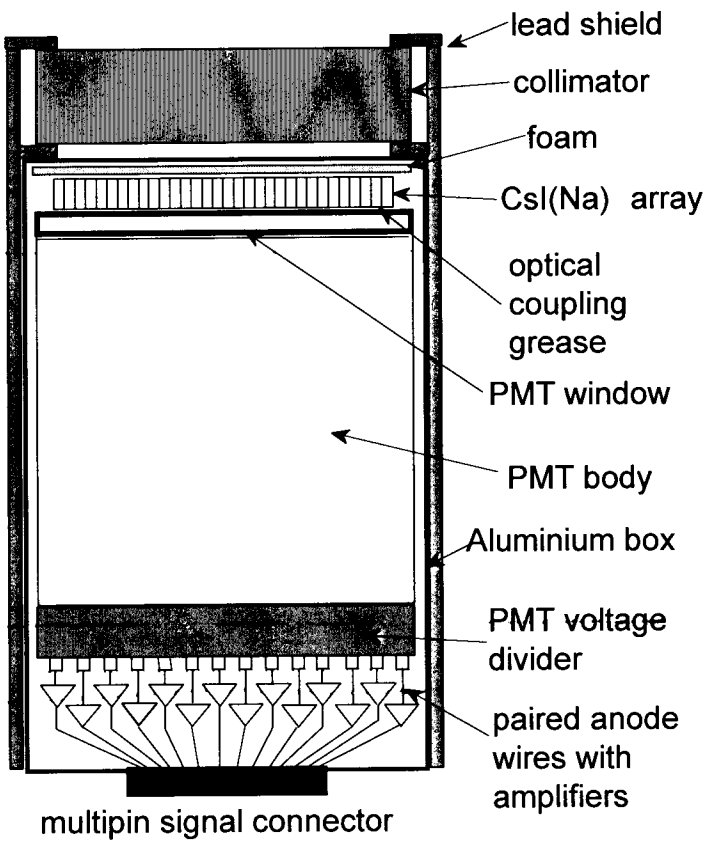

Figure 3. Cross sectional view of the 5 inch diameter R3292-02 PSPMT coupled to the CsI(Na) crystal array.

The signal from the last dynode of the PSPMT is inverted and amplified before passing through the discriminator electronics so as to detect an event and determine if the signal amplitude is above a desired background and noise threshold, and to generate a 1 μsec wide gate to FERA ADCs. When the detector is operated in coincidence mode the signal from the anode of the coincidence PMT is ANDed with the shaped dynode signal from the PSPMT. The data acquisition system use FERA ADCs from LeCroy and a Power Macintosh 8100 workstation as the host computer running control software we developed using the Kmax data acquisition system from Sparrow Corporation.

3.2 CsI(Na) Scintillating Crystal Array

The individual CsI(Na) crystal elements are resolved using the same truncated center of gravity technique discussed earlier. The real-time data processing developed and implemented using the Kmax data acquisition system treats the output of each crystal region individually to correct for crystal-to-crystal scintillation output variations as well as the local PSPMT gain variations (see figure 4 for a raw flood image and a projection of the center row). The individual crystals-pixels show variations in light output depending on their origin from the crystal boule and variations in surface treatment.

Individual crystals are easily resolved as can be seen in a the ^{125}I image shown in the left half of Figure 4. The image was obtained using a ^{125}I point source placed ~10 cm above the CsI(Na) array.

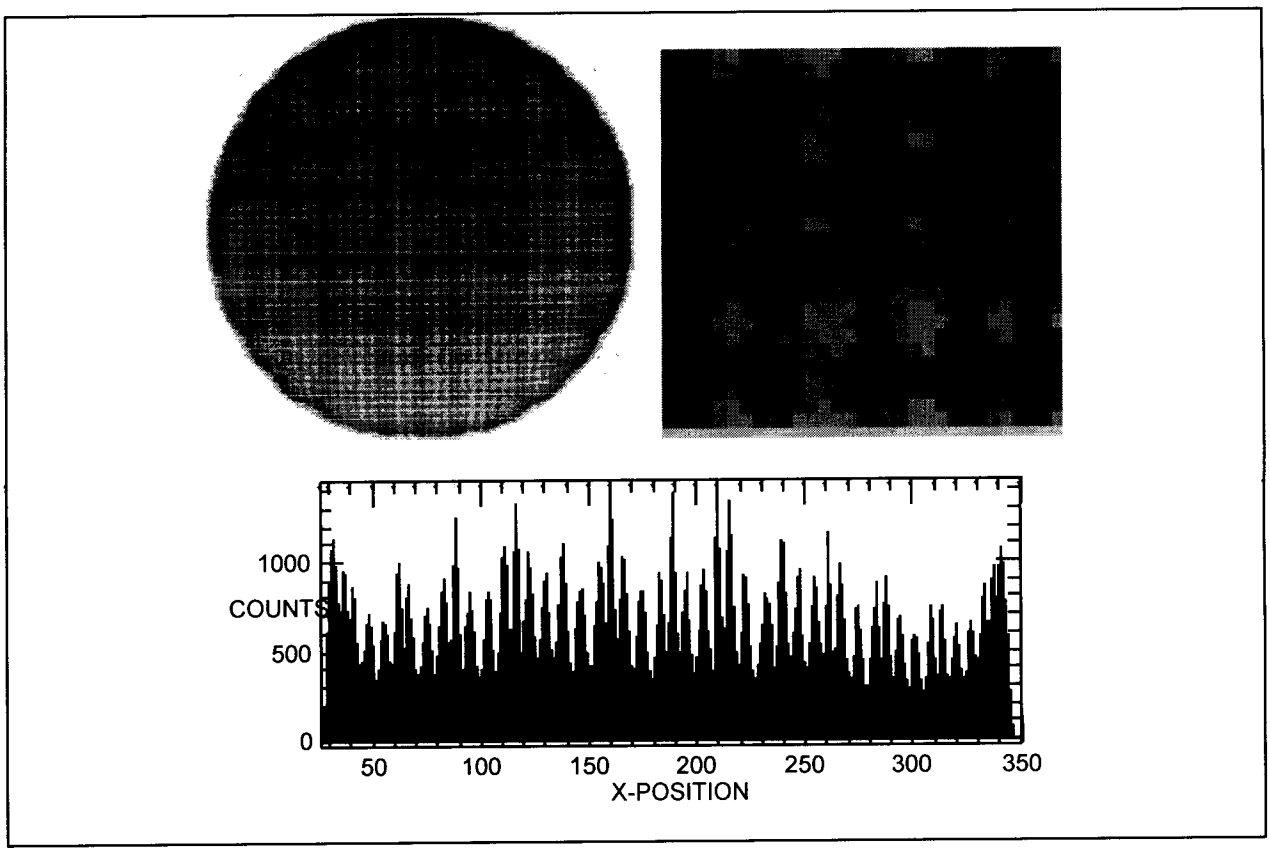

Figure 4. The full flood image of the crystal array is shown in the top left portion of this figure. This was done by using a ^{125}I point source placed ~10 cm above the CsI(Na) crystal array. An enlargement of the central region of the image is in the top right. The histogram in the lower half of the figure is a projection of a single row. The data was taken in coincidence mode. Over 95% of the crystals are resolved.

A conventional 5 inch diameter photomultiplier with a NaI(Tl) crystal made by Isotopes Products Laboratories was used as the coincidence detector. The NaI(Tl) crystal is 121 mm in diameter, 3 mm thick with a 1 mm quartz window and a 0.3 mm aluminum entrance window. This coincidence detector was placed in near contact with the ^{125}I source. In the bottom half of Figure 4 is a projection through one row of crystals showing the isolation of the 2 x 2 mm^2 individual crystals. The pulse height spectrum for this image is shown in Figure 5. This histogram is generated by summing the individual anode outputs from both axes.

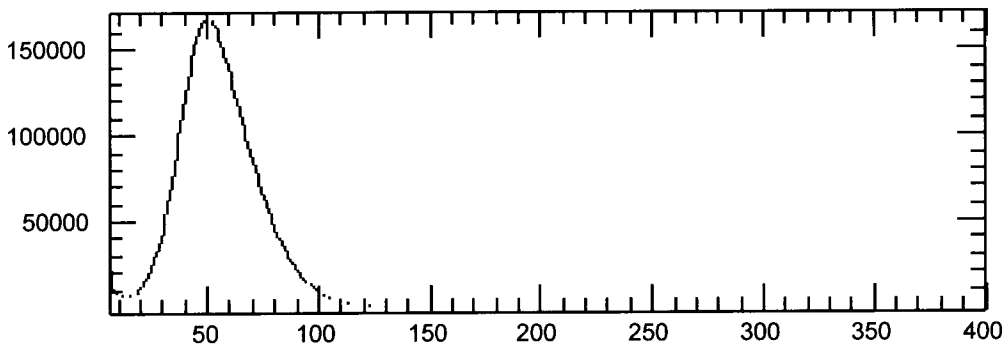

Figure 5. Pulse height spectrum (arbitrary units) from the figure 1 image taken in coincidence mode.

3.3 Crystal Array Mapping

Images obtained with the PSPMT exhibit distorted crystal positions because of spatial non-uniformity of response in the PSPMT. Since the relative position of each crystal is known and the crystals can be defined in the raw image, a distortion correction is easily achieved by mapping the data identified to belong to a particular crystal into that crystal's appropriate pixel in the corrected image. Figure 6 shows the points that have been determined to mark individual crystal region corners. They have been obtained using a flood image and after the borders of each region were defined.

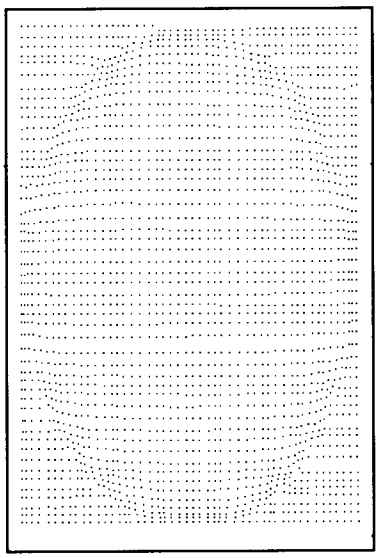

Figure 6. Map of crystal regions. Each crystal region is marked by four dots, one at each corner. The crystal array is actually a circle formed from an array of square crystal elements, "false" filler crystal were marked to simplify the real time look-up table computer algorithm.

We investigated the ability to image ^{125}I labeled melatonin that has concentrated in various sites in a live mouse. Melatonin is known to have binding sites in the brain and other organs of an adult mouse [14]. In Figure 7 are examples of a raw and a corrected image which were acquired in singles mode so there is much background. A 1 cm thick high resolution parallel hole lead collimator core was placed in front of the CsI(Na) array to obtain planar images of the distribution of ^{125}I in the body of the mouse.

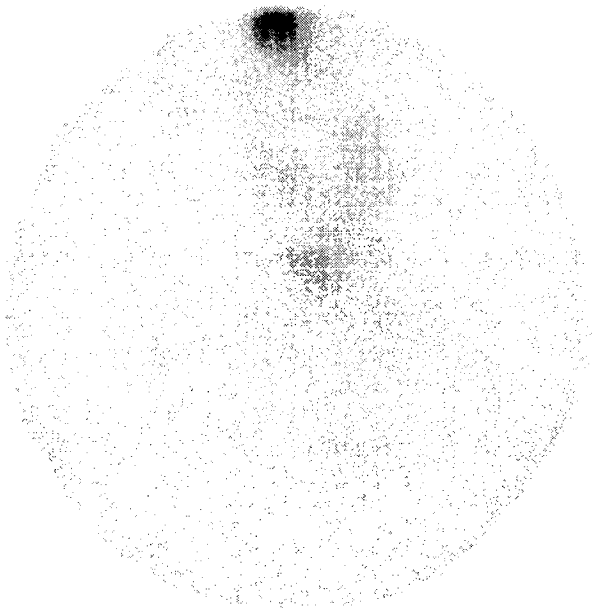

Figure 7. This is the raw image obtained using the CsI(Na) array. In this image it is possible to see individual crystals of the array particularly in the area of the hot spot at the top of the image which corresponds to the mouse's bladder. The mouse was positioned with its head pointing downward and the tip of the mouse's nose is 1/3 of the way up from the bottom of the figure.

The imaging information contained in Figure 7 is sorted and mapped on a crystal by crystal bases for the appropriate location and energy window. The results of this real time processing for position and energy is shown in Figure 8. A energy window of 20% was used to form the image.

Figure 8. This is the corrected image obtained using the data in Figure 7 and applying the crystal boundary information shown in Figure 6.

The image shows the melatonin distribution in the mouse. A dose of approximately 11 μCi (0.06 ml) ^{125}I labeled melatonin obtained from Amersham Inc. was injected into a tail vein of a 23 gm male *Peromyscus maniculatus* mouse. The mouse was anesthetized with 0.35 ml of 4% chloral hydrate and imaging was started 60 minutes after injection of the ^{125}I labeled melatonin. Total image acquisition time was 10 minutes.

3.4 Coincidence Imaging

We have determined that the implementation of the coincidence detection requirement for imaging the concentration of ^{125}I to be most advantageous for the case where small amounts of ^{125}I (<10 μCi) were attempted to be imaged over acquisition times of 10 to 20 minutes. We found it most useful to be able to switch between the two modes of data acquisition to optimize the imaging results. In Figure 9 is an image of a ~75 μCi ^{125}I phantom source imaged in singles and coincidence mode with a 3 minute acquisition time for each. One can see that much of the background is reduced.

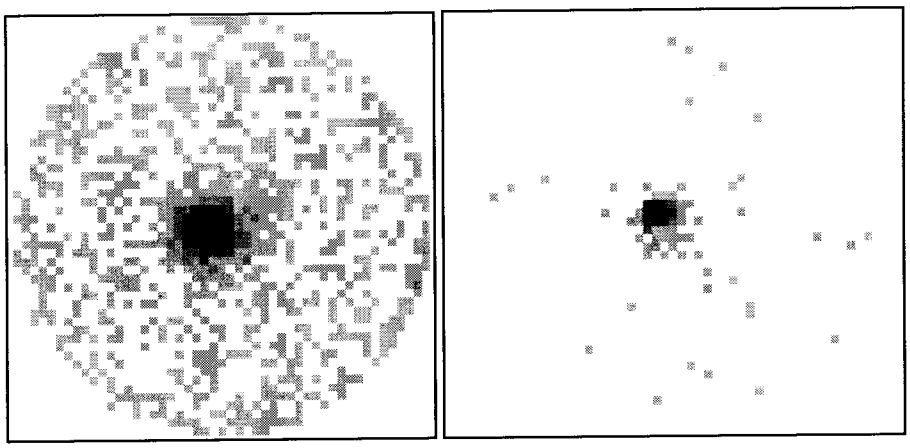

Figure 9. In this figure we show an image of a ~75 μCi ^{125}I phantom taken in singles mode (left) and coincidence mode (right). Both images represent 3 minutes of data acquisition.

4. Continuing Developments

The new detector system we are constructing is again based on a CsI(Na) crystal array coupled to the 5 inch diameter Hamamatsu R3292-02 PSPMT. The new scintillator array is 110 mm in diameter and each element is 1.0 x 1.0 mm^2 in area and 3 mm thick with a 0.2 mm white diffusive dead space between each element. We are designing a gantry to hold the PSPMT such that it would be possible to rotate the detector system around the mouse being imaged in order to collect enough projections to reconstruct the three dimensional image of the ^{125}I source distribution in an animal. The detection of the coincidence radiation will be achieved by "boxing" in the mouse with four large area crystal scintillators. The light from these coincidence crystal scintillators will be directed to a traditional PMT via light guides or light guide fibers.

We are in now in the early stages of using our detector system to test the ability of imaging gene expression in live mice using antisense RNA techniques. A collimator will be needed to achieve an image formation on the PSPMT. Since we are using low energy gamma-rays the collimator design is less of a challenge than would be the case for higher energy gammas such as with ^{99m}Te

5. Acknowledgments

We would like to express our appreciation to Dr. Paul Heideman of the Biology Department of the College of William and Mary for his assistance with the melatonin study. We also thank Dr. Simon Cherry of the UCLA Crump Institute for his many helpful suggestions. We thank Tom Carstens of Jefferson Lab for the design and assembly of the amplifier boards used in this detector.

The Southeastern Universities Research Association (SURA) operates the Thomas Jefferson National Accelerator Facility for the United States Department of Energy under contract DE-AC05-84ER40150. The project was supported in part by NSF grant # IBN9602865.

6. References

1. K.G. Peters, P.S. Rao, B.S. Bell & L.A. Kindman, "Green Fluorescent Fusion Proteins: Powerful Tools for Monitoring Protein Expression in Live Zebrafish Embryos", *Developmental Biology*, no. 171 pp. 252-257, 1995.
2. M.K. Dewanjee, A.K. Ghafouripour, M. Kapadvanjwala, E.L. Oates, A. Krishan, D.M. Lopez, A.N. Serafini & G.N. Sfakianakis, "Radiolabeled Antisense Oligodeoxynucleotides: In Vitro and In Vivo Application", *Jour. of Clinical Immunoassay*, vol 16, no 4, p. 276, 1993.
3. M.K. Dewanjee, A.K. Ghafouripour , M. Kapadvanjwala, S. Dewanjee, A.N. Serafini, D.M. Lopez & G.N. Sfakianakis, "Noninvasive Imaging of c- *myc* Oncogene Messenger RNA with Indium-111-Antisense Probes in a Mammary Tumor-Bearing Mouse Model" , *Journal of Nuclear Medicine*, vol. 35, no. 6, June 1994.
4. M.K. Dewanjee, "Radiolabeled Antisense Probes: Diagnostic and Therapy", *Diagnostic Oncology*, 3:189, 1993.
5. M.T. Madsen, W. Chang, R.D. Hichwa, "Spatial resolution and count density requirements in brain SPECT imaging", *Phys Med Biol* (P6J), 37 (8): 1625-36, Aug 1992.
6. J.G. Tjuvajev, G. Stockhammer, R. Desai, H. Uehara, K. Watanabe, B. Gansbacher and R.G. Blasberg, "Imaging the expression of transfected genes *in vivo*", *Cancer Res (CNF),* 55 (24): 6126-32, Dec 15, 1995.
7. J. G. Tjuvajev, R. Finn, K. Watanabe, R. Joshi, T. Oku, J. Kennedy, B. Beattie, J Koutcher, S. Larson and R. G. Blasberg, "Noninvasive imaging of herpes virus thymidine kinase gene transfer and expression: a potential method for monitoring clinical gene therapy," *Cancer Res (CNF)*, 56 (18): 4087-95, Sep 15, 1996.
8 NEN®Research Products Catalog, DuPont NEN, June 1994.
9 Lederer CM., and Shirley VS, Table of Isotopes, 7th ed., John Wiley & Sons, Inc., New York, 1978.
10 Drukier AK, "MultiPhoton Detection", Workshop on Ultrahigh Sensitivity Quantification Methodologies and Instrumentation for Biomedical Applications , NIST, Gaithersburg, MD, July, 1995.
11. A.G. Weisenberger, E. Bradley, S. Majewski and M. Saha, "Development of a Novel Radiation Imaging Detector System for *In Vivo* Gene Imaging in Small Animal Studies", *Conference Record of the 1996 IEEE Medical Imaging Conference* , pp. 1201-1205, 1996.
12. D. Steinbach, S. Majewski, M. Williams, B. Kross, A.G. Weisenberger and R. Wojcik, "Development of a Small Field of View Scintimammography Camera Based on a YAP Crystal Array and a Position Sensitive PMT", Conference Record of the 1996 IEEE Medical Imaging Conference, pp. 1251-1256, 1996.
13 A. Truman, A.J. Bird, D. Ramsden and Z. He, " Pixellated CsI(Tl) arrays with position-sensitive PMT readout", *Nuclear Instruments and Methods in Physics Research A* , 353(1994) pp. 375-378, 1994.
14. P. J. Morgan, P. Barrett, H. E. Howell and R. Helliwell, "Melatonin Receptors: Localization, Molecular Pharmacology and Physiological Significance," *Neurochem Int*. vol 24, no. 2, pp. 101-146, 1994.